Part IV. Polarization & Magnetic Fields

https://doi.org/10.1017/S0074180900222717 Published online by Cambridge University Press

Cosmic MASERs: From Protostars to Blackholes
IAU Symposium, Vol. 206, 2002
V. Migenes and M. J. Reid, eds

Observational studies of maser polarization

Athol Kemball
National Radio Astronomy Observatory, P.O. Box 0, Socorro NM 87801, USA

Abstract. This paper reviews observational studies of maser polarization, with particular reference to observational results reported in the intervening eight years since the last maser conference (Clegg & Nedoluha 1993). The scientific role of maser polarization observations is discussed and the theoretical interpretation of such data is considered. Recent observational results are presented for several common maser transitions, including OH, H_2O, and SiO.

1. Introduction

Maser observations are important both for what they reveal about intrinsic maser properties as well as for what they reveal about the physical properties of the maser environment. Masers are excellent astrophysical probes in this sense, primarily because of their compactness, high brightness and ubiquity in a range of astrophysical environments, including star-forming regions and late-type circumstellar shells. Polarization observations add fundamental additional information about the radiation field and thus expand the role masers can play as probes of their local conditions. Masers are often highly circularly or linearly polarized in a range of common molecular transitions. Taken in concert with a theory of maser polarization propagation, polarization observations allow inference of the B-field magnitude, orientation, spatial distribution, energy density and dynamical influence. In addition, the compactness and high brightness temperature of individual maser components allows these properties to be measured at milliarcsecond (mas) spatial resolution using VLBI techniques. At high resolution, maser polarization can also be used to tag or identify individual maser components in kinematic studies, such as proper motion. Polarization observations also help to refine and verify theoretical models for the transport of polarized maser radiation.

In the period covered by this paper, maser polarization observations have played a role in improving the understanding of a range of scientific problems. These include the morphology and magnitude of asymptotic giant branch (AGB) stellar magnetic fields, as well as the kinematics and dynamics of AGB circumstellar material. Maser polarization observations have also helped to elucidate the B-field structure and shock structure of star-forming regions and supernova remnants. In addition, they have allowed further investigation of the possible alignment of local star-forming and galactic magnetic fields.

The organization of this paper is as follows. In Section 2, the theoretical interpretation of maser polarization observations is discussed. Section 3 describes observational techniques, and Sections 4 through 7 consider observational results for several common maser transitions. A summary is provided in Section 8.

2. Maser polarization theory

The Zeeman effect arises from the breaking of the degeneracy of quantum magnetic substates in an applied magnetic field. The magnitude of this coupling is substantially different for paramagnetic and non-paramagnetic molecules, as expressed by the ratio of the Bohr magneton $\mu_B = \frac{e\hbar}{2m_e c}$ to the nuclear magneton $\mu_N = \frac{e\hbar}{2m_n c}$, given as $\mu_B \sim 10^3 \mu_N$. In this expression, m_e is the electron mass, m_n the nucleon mass, e the electron charge, $\hbar$ the Planck constant and c the speed of light. This ratio defines the overall qualitative polarization properties of any given maser transition.

The propagation of an underlying Zeeman pattern along a maser amplification path differs from the thermal case due to the intrinsic stimulated emission process and the range of additional underlying physical parameters which may affect the polarization transport. The theoretical problem is framed by constructing the density matrix evolution and maser radiation transfer equations including Zeeman terms (Goldreich, Keeley & Kwan 1973). A fundamental parameter, which defines whether the magnetic transitions overlap in frequency or are well-separated, is the splitting ratio, $r_Z = \frac{\Delta\nu_Z}{\Delta\nu_D}$ (Elitzur 1996), where $\Delta\nu_Z$ is the Zeeman splitting, and $\Delta\nu_D$ is the Doppler line-width. Additional parameters which may influence polarization propagation include the degree of saturation, the relaxation rate, transition spin, Faraday rotation, pumping isotropy and the presence or absence of magnetic field or velocity gradients along the maser path, amongst other factors. By implication, the inverse problem of deducing physical properties in a masing region based on observed net polarization can be a difficult challenge. This is the key theoretical question which is faced when interpreting maser polarization observations.

The primary observables in maser polarization observations are the Stokes profiles in I, Q, U and V across the line, which encode the underlying frequency shifts of the constituent Zeeman components, optionally spatially resolved for individual maser components. The polarization information may alternatively be expressed as the electric vector position angle χ, degree of linear polarization m_l and the degree of circular polarization m_c. In general, m_c can be used to estimate the B-field magnitude, and χ the projected magnetic field orientation with respect to the line of sight.

For the case of large splitting, $r_Z > 1$, the Zeeman pattern is resolved and there are no theoretical ambiguities. In this case the Zeeman components are well-separated and resolved. For $\Delta m_F = \pm 1$, the emitted radiation components are $\sigma^{\pm}$ components, circularly polarized perpendicular to the magnetic field B. For $\Delta m_F = 0$, the emitted radiation components are π components, linearly polarized along B. For an arbitrary incident angle θ between the magnetic field and the propagation direction, the resultant components are elliptically polarized for $\theta < \frac{\pi}{2}$ (with an axis ratio $\cos\theta$), and are linearly polarized for

https://doi.org/10.1017/S0074180900222717 Published online by Cambridge University Press

$\theta = \frac{\pi}{2}$. The velocity shift of the σ-components is $\Delta u = \frac{g\mu Bc \cos\theta}{h\nu_0}$, where ν_0 is the transition frequency, g the Lande factor and B the magnetic field magnitude (Lis, Goldsmith & Predmore 1989).

For the case of small splitting, $r_Z < 1$, the Zeeman components overlap in frequency. Theoretical work admits both Zeeman (Elitzur 1995; Elitzur 1996; and references therein) and non-Zeeman (Watson 1994; Wiebe & Watson 1998; and references therein) interpretations, with considerable implications for inferred B-field magnitudes. In the standard Zeeman interpretation for this case $B \propto m_c$, with an orientation relative to the projected B-field that is parallel for $\theta < 55°$ and perpendicular for $\theta > 55°$ (Elitzur 1992).

3. Observational techniques

There are significant scientific advantages in taking maser polarization observations at the highest spatial resolution, so that the full Stokes profile over velocity can be measured separately for each spatially resolved maser component. These data can be taken using the technique of spectral line interferometric polarimetry. Such observations require calibration of the complex antenna gain and instrumental polarization response for each sampled polarization. At the highest VLBI spatial resolution and at millimeter wavelengths, calibration may require a simultaneous estimate of the instrumental effects and the source polarization structure using a variant of self-calibration. This problem has become more tractable in recent years due to both hardware and algorithm improvements (Kemball, Diamond and Cotton 1995; Leppänen, Zensus & Diamond 1995; and references therein). The algorithm advances derive from the the first maser polarization VLBI studies (Moran et al. 1978; Reid et al. 1980).

Once a calibrated full polarization image cube has been produced, a common data analysis requirement is to extract the Zeeman component velocity splitting for a given component Stokes profile. For the case of small Zeeman splitting, the Stokes V profile has a characteristic asymmetric S-profile formed by the addition of two offset Gaussian line profiles of opposite circular polarization. In this regime, the technique used in thermal Zeeman studies can be used as an estimator of the component separation, as expressed in the formalism (Troland & Heiles 1982):

$$V(\nu) = \alpha \frac{dI(\nu)}{d\nu} + \beta I(\nu)$$

where ν is frequency, α is the splitting factor and β is a differential gain factor. Sault et al. (1990) performed a statistical analysis of this estimator. Broadly summarized, they found it applicable in the case when $r_Z < 0.1$ and there are more than ten samples per line-width across the profile. This argues strongly for high frequency resolution in maser polarization observations.

4. OH (hydroxyl) masers

The Zeeman splitting is tabulated for common OH maser transitions in Table 1. For hydroxyl masers the Zeeman splitting ratio is intermediate or large, i.e.

$r_Z > 1$ or $r_Z \sim 1$. As discussed above, for the case of large r_Z, there is no theoretical ambiguity concerning the implied B-field.

Table 1. OH Zeeman parameters

Transition	Rest frequency (MHz)	Zeeman splitting (km s^{-1} mG^{-1})
$^2\Pi_{\frac{3}{2}}$, $j = \frac{3}{2}$, $F = 1 - 2$	1612.231	0.236
$^2\Pi_{\frac{3}{2}}$, $j = \frac{3}{2}$, $F = 1 - 1$	1665.401	0.590
$^2\Pi_{\frac{3}{2}}$, $j = \frac{3}{2}$, $F = 2 - 2$	1667.358	0.354
$^2\Pi_{\frac{3}{2}}$, $j = \frac{3}{2}$, $F = 2 - 1$	1720.533	0.236
$^2\Pi_{\frac{3}{2}}$, $j = \frac{5}{2}$, $F = 2 - 2$	6030.739	0.079
$^2\Pi_{\frac{3}{2}}$, $j = \frac{5}{2}$, $F = 3 - 3$	6035.085	0.056
$^2\Pi_{\frac{3}{2}}$, $j = \frac{7}{2}$, $F = 4 - 4$	13441.371	0.018

References: Davies et al. (1974); Lang (1986); Baudry & Diamond (1998)

4.1. Stellar OH masers

Zeeman observations of stellar OH masers around late-type stars allow direct estimation of the stellar B-field magnitude at the position of the OH masers in the circumstellar shell. Assuming a radial dependence for the B-field between r^{-2} and r^{-3} (Reid 1990), these measurements allow an approximate extrapolation of the B-field magnitude to the surface of the photosphere. Recent measurements of this type are listed in Table 2.

Table 2. OH: Stellar B-field estimates

Source	Telescope	OH transition (MHz)	B_{shell} (mG)	B_{star} (G)	Ref.
IRC10420	VLA	1612, 1665	0.18-15	3000	[1]
IRC10420	EVN	1612	1-3	10-30	[2]
IRAS 17150-3224	Nancay	1665	0.3	160	[3]
W Hya	MERLIN	1667	0.6	4	[4]

References: [1] Nedoluha & Bowers (1992); [2] Kemball (1993); [3] Hu et al. (1993); [4] Szymczak, Cohen & Richards (1998)

Zeeman studies of stellar OH masers often find an organized spatial Stokes V morphology, suggesting a globally ordered field (Zell & Fix 1996; Szymczak et al. 1998; Szymczak, Cohen & Richards 1999).

4.2. OH masers in star-forming regions

Zeeman observations of OH masers in star-forming regions yield B-field magnitudes that are fairly uniform and consistent with earlier results. Recent measurements of this type are listed in Table 3.

OH Zeeman observations also allow an estimate of the B-field direction, as described above. Results obtained from star-forming regions over a range

https://doi.org/10.1017/S0074180900222717 Published online by Cambridge University Press

Table 3. OH: Star-forming region B-field estimates

Source	Telescope	OH transition (MHz)	B (mG)	Ref.
Survey	Parkes	1665, 6035	1-10	[1]
Survey	Effelsberg	6031, 6035	3-8	[2]
W3(OH)	EVN	6031, 6035	2-15	[3]
W3(OH)	VLBA	13441	6-11	[4]
G34.3+0.2	US VLBI	1665, 1667	1-7	[5]
G34.3+0.2	VLBA	1665, 1667	1-8	[6]

References: [1] Caswell & Vaile (1995); [2] Baudry et al. (1997);
[3] Desmurs et al. (1998); [4] Baudry & Diamond (1998);
[5] Zheng, Moran & Reid (2000); [4] Zheng, Reid & Moran (2000);

of galactic longitudes have been used to explore the possible alignment of local B-fields with the galactic field (Baudry et al. 1997).

Observed Zeeman pairs in both circumstellar and star-forming regions seldom conform with the expected theoretical line ratios and intensities. They are frequently asymmetrical in velocity and may be incompletely formed. This could be intrinsic or influenced by inhomogeneities in the local masing conditions for each Zeeman component. In addition, the linear polarization is generally lower than would be expected from a single π component in a fully-resolved Zeeman pattern. This could possibly be intrinsic, but is reasonably assumed to be caused by local Faraday depolarization.

4.3. Megamasers and supernova remnants

ATCA observations of four megamasers at 1667 MHz found no Zeeman detections ($B < 3-5$ mG) (Killeen et al. 1996). For information concerning studies of 1720 MHz OH masers towards supernova remnants, which is a well-established field, see Green (2001), Yusef-Zadeh (2001) and Brogan (2001) in these proceedings.

5. Water masers

The water molecule is non-paramagnetic and has overlapping hyperfine components in the 22 GHz maser transition. The Zeeman splitting ratio is $r_Z \sim 10^{-3} - 10^{-4}$, and this transition has very low circular polarization ($m_c < 0.1\%$) (Fiebig & Güsten 1989). Polarization VLBI observations of the water masers towards the star-forming region W51M by Leppänen, Liljeström & Diamond (1998) show that the masers may be substantially linearly polarized ($\sim 35\%$), and that they trace the local shock structure. Water maser flares, such as those in Orion, can be very highly linearly polarized (Abraham & Vilas Boas 1994) as described elsewhere in these proceedings (Horiuchi 2001).

Sarma, Troland & Romney (2001) have reported the first VLBI detection of a Zeeman Stokes V component profile towards a star-forming region (W3 IRS 5), and report a line-of-sight B-field magnitude of ~ 40 mG for this source. Vlemmings et al. (2001; these proceedings) report a similarly ground-breaking detection of a VLBI Zeeman component for a circumstellar water maser. Observations of this type have great potential for establishing tighter constraints on the radial dependence of stellar magnetic fields.

6. SiO masers

SiO is a simple rotor and is non-paramagnetic. It exhibits maser action in several vibrationally excited rotational transitions, e.g. $\nu = 1, J = 1 - 0$ (43.122027 GHz), $\nu = 2, J = 1 - 0$ (42.820539 GHz), $\nu = 1, J = 2 - 1$ (86.243350 GHz). The Zeeman splitting ratio for the $\nu = 1, J = 1 - 0$ transition in a B-field of 10-100 G is $r_Z \sim 0.005 - 0.05$.

Previous studies have detected high integrated linear polarization (McIntosh et al. 1989), and modest circular polarization $m_c \sim 10\%$ (Barvainis, McIntosh & Predmore 1987). The integrated fractional linear polarization and electric vector position angle are comparable for simultaneous $\nu = 1,\ J = 1 - 0, J = 2 - 1$ and $J = 3 - 2$ transitions (McIntosh & Predmore 1993).

Full VLBI polarimetry in Stokes (I, Q, U, V) at 43 GHz is now possible using forms of polarization self-calibration on the VLBA (Kemball et al. 1995; Leppänen et al. 1995). Observations of this type reveal an organized global polarization morphology (Kemball & Diamond 1997; Desmurs et al. 2000). Higher circular polarization is measured at VLBI resolution than from integrated single-dish studies. For the VLBI studies, $m_c \sim 30 - 40\%$ for isolated features, with a median of $\sim 3 - 5\%$ (Kemball & Diamond 1997). The stellar SiO masers show fine-scale polarization structure at sub-milliarcsecond resolution. Both Zeeman and non-Zeeman interpretations of the SiO maser polarization properties are possible as this is the small-splitting case. Assuming a Zeeman interpretation, B-field magnitudes at the Gauss level are implied at the position of the SiO masers in the extended stellar atmosphere. However, non-Zeeman interpretations suggest a field order of magnitudes smaller, and explain the ordered global polarization by invoking the preferred axis introduced by radiative pumping (Desmurs et al. 2000). Observations of larger source samples will help to resolve this important question.

7. Other transitions

Methanol polarization studies are described by Elligson (2001; these proceedings).

A B-field estimate has also been obtained from observations of the H30α recombination line maser towards MWC 349 at 232 GHz using the IRAM 30m telescope (Thum and Morris 1999), who determined a B-field estimate of ~ 22 mG for this source.

8. Summary

In the period covered by this paper, maser polarization observations have provided important new information on the physical properties of a variety of different astrophysical environments. In addition, they have provided unique measurements of the magnetic fields in these regions and their dynamical influence. The technical obstacles are now greatly reduced for full polarization interferometry at high spatial resolution. New instruments, such as ALMA, EVLA, and eMERLIN, will reduce these obstacles still further.

The scientific value of maser polarization studies in the future will be enhanced by larger source samples, higher spatial, velocity and time resolution, simultaneous observations of a range of excited transitions, better modeling of external factors (such as velocity and magnetic field gradients), and independent measurements of B-field properties in these regions. The future scientific potential of observations of this type remains considerable.

References

Abraham, Z. & Vilas Boas, J. W. S. 1994, A&A, 290, 956

Barvainis, R., McIntosh, G., & Predmore, C. R. 1987, Nature, 329, 613

Baudry, A., Desmurs, J. F., Wilson, T. F., & Cohen, R. J. 1997, A&A, 325, 255

Baudry, A. & Diamond, P. J. 1998, A&A, 331, 697

Caswell, J. L. & Vaile, R. A. 1995, MNRAS, 273, 328

Clegg, A. W. & Nedoluha, G. E. 1993, Astrophysical Masers (Berlin: Springer-Verlag)

Davies, R. D. 1974, in Galactic Radio Astronomy, ed. F. J. Kerr & S. C. Simonson III (IAU), 275

Desmurs, J. F., Baudry, A., Wilson, T. F., Cohen, R. J., & Tofani, G. 1998, A&A, 334, 1085

Desmurs, J. F., Bujarrabal, V., Colomer, F., & Alcolea, J. 2000, A&A, 360, 189

Elitzur, M. 1992, Astronomical Masers (Dordrecht: Kluwer)

Elitzur, M. 1995, ApJ, 440, 345

Elitzur, M. 1996, ApJ, 457, 415

Fiebig, D. & Güsten, R. 1989, A&A, 214, 333

Goldreich, P., Keeley, D. A., & Kwan, J. Y. 1973, ApJ, 179, 111

Hu, J. Y., Slijkhuis, S., Nguyen-Q-Rieu, & de Jong, T. 1993, A&A, 273, 185

Kemball, A. J. 1993, Ph.D. thesis, Rhodes University

Kemball, A. J., Diamond, P. J., & Cotton, W. D. 1995, A&AS, 110, 383

Kemball, A. J. & Diamond, P. J. 1997, ApJ, 481, L111

Killeen, N. E. B., Staveley-Smith, L., Wilson, W. E., & Sault, R. J., 1996, MNRAS, 280, 1143

Lang, K. R. 1986, Astrophysical Formulae (Heidelberg: Springer-Verlag)

Leppänen, K. J., Zensus, J. A., & Diamond, P. J. 1995, AJ, 110, 2479

Leppänen, K., Liljeström, T., & Diamond, P. 1998, ApJ, 507, 909

Lis, D. C., Goldsmith, P. F., & Predmore, C. R. 1989, ApJ, 341, 823

McIntosh, G. C., Predmore, C. R., Moran, J. M., Greenhill, L. J., Rogers, A. E. E., & Barvainis, R. 1989, ApJ, 337, 934

McIntosh, G. C. & Predmore, C. R. 1993, ApJ, 404, L71

Moran, J. M., Reid, M. J., Lada, C. J., Yen, J. L., Johnston, K. J., & Spencer, J. H. 1978, ApJ, 224, L67

Nedoluha, G. E. & Bowers, P. F. 1992, ApJ, 392, 249

Reid, M. J., Haschick, A. D., Burke, B. F., Moran, J. M., Johnson, K. J., & Swenson, G. W. 1980, ApJ, 239, 89

Reid, M. J. 1990, in Galactic and Intergalactic Magnetic Fields, ed. R. Beck et al. (Netherlands: IAU), 21

Sarma, A. P., Troland, T. H., & Romney, J. D. 2001, ApJ, 554, L217

Sault, R. J., Killeen, N. E. B., Zmuidzinas, J., & Loushin, R. 1990, ApJS, 74, 437

Szymczak, M., Cohen, R. J., & Richards, A. M. S. 1998, MNRAS, 297, 1151

Szymczak, M., Cohen, R. J., & Richards, A. M. S. 1999, MNRAS, 304, 877

Thum C. & Morris, D. 1999, A&A, 344, 923

Troland, T. H. & Heiles, C. 1982, ApJ, 252, 179

Watson, W. D. 1994, ApJ, 424, L37

Wiebe, D. S. and Watson, W. D. 1998, ApJ, 503, L71

Zell, P. J. & Fix, J. D. 1996, AJ, 112, 252

Zheng, X. W., Moran, J. M., & Reid, M. J. 2000, MNRAS, 317, 192

Zheng, X., Reid, M. J., & Moran, J. M. 2000, A&A, 357, L37

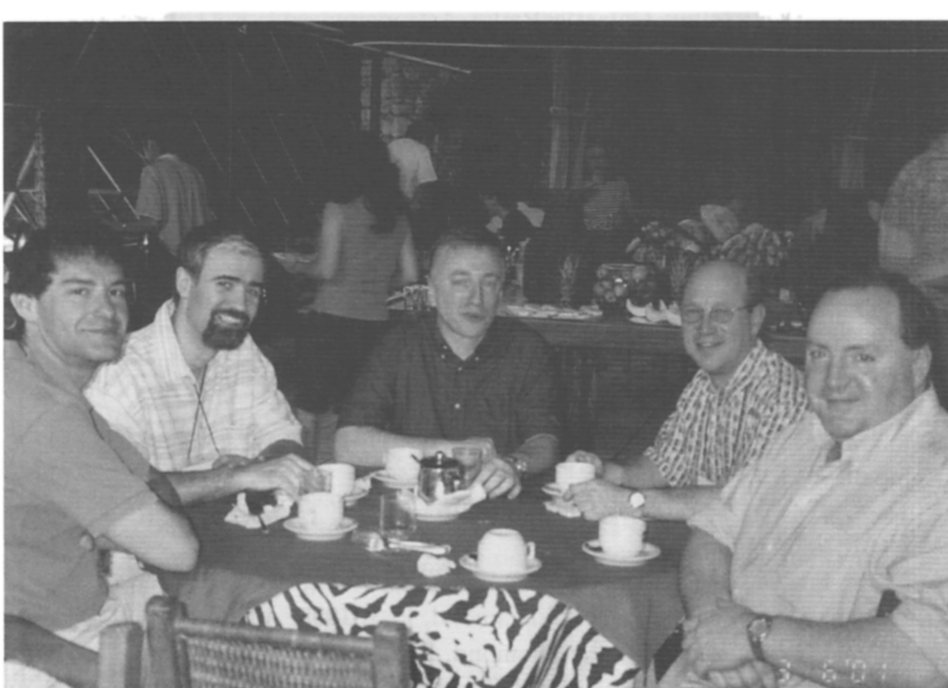

https://doi.org/10.1017/S0074180900222717 Published online by Cambridge University Press